Running title: Glioblastoma cell death induced by HRD1 inhibition

Inhibition of enzymatic activity of HRD1 results in death of cells derived from glioblastoma multiforme, neuroblastoma, and normal astrocytes

Jaroslava Guzikova[1], Monika Liskova[1], Lubos Hudak[1], Maria Brodnanova[2], Andrea Evinova[2], Jozef Hatok[1], Peter Racay[1,*]

[1]Department of Medical Biochemistry, Comenius University in Bratislava, Jessenius Faculty of Medicine in Martin, Martin, Slovakia; [2]Biomedical Center Martin, Comenius University in Bratislava, Jessenius Faculty of Medicine in Martin, Martin, Slovakia

*Correspondence: peter.racay@uniba.sk

The aim of the present study was to examine the impact of LS-102, an inhibitor of enzymatic activity of HRD1 that is an essential E3 ubiquitin ligase of endoplasmic reticulum associated degradation (ERAD) on survival of the human cell lines derived from glioblastoma multiforme (GBM), neuroblastoma, and astrocytes. We have also examined molecular responses to HRD1 inhibition with a focus on proteins playing an essential role in unfolded protein response (UPR) and ERAD. In addition, activation of IRE1α documented by XBP1 splicing was investigated. Finally, we have examined the impact of LS-102 on p53 expression in GBM cells. Inhibition of HRD1 enzymatic activity results in cell death of all tested cells. With respect to GBM cells, U87 cells are more sensitive to LS-102 as T98G cells. Cells of cell lines derived from normal astrocytes K1884 exhibit the highest sensitivity to LS-102 among all cell types used in the study while NHA cells are the most resistant. Sensitivity of neuroblastoma SH-SY5Y cells to LS-102 is comparable to the sensitivity of U87 cells. In GBM cells, inhibition of HRD1 results in induction of the expression of proteins playing an essential role in UPR and ERAD (HRD1, SEL1L, and GRP78). XBP1 splicing induced by HRD1 inhibition was documented in T98G and K1884 cells. We did not observe induction of p53 expression in U87 cells. Since LS-102 induces cell death of normal astrocytes, it is not a candidate for the testing of its potential use as an antitumor treatment of GBM.

Glioblastoma multiforme (GBM) is the most common and the most aggressive primary brain tumor [1]. Despite to the current treatments; which include surgical resection, chemotherapy using temozolomide and radiotherapy; tumor recurrence occurs in almost all patients resulting in median survival of less than 15 months [2]. GBM diffusely infiltrates the adjacent brain tissue [3] and rarely spreads outside the central nervous system [4]. Diffuse infiltration into the normal brain parenchyma is a hallmark of GBM and underlies recurrence by precluding complete surgical resection [5, 6]. Thus, the development of new therapy of GBM based on cytotoxic drugs represents great challenge of current biomedical research.

49 In order to maintain high proliferation rate, both DNA and protein synthesis is elevated in tumor
50 cells. In addition to deregulated translation, deregulated/overloaded polypeptide processing,
51 including polypeptide modification and folding located in endoplasmic reticulum (ER) could
52 contribute to the cancer progression [7, 8]. All these factors along with limited oxygen and nutrient
53 supply to the growing tumor [7, 9] result in ER stress and initiation of the unfolded protein response
54 (UPR) [7, 8]. Aberrant folding of proteins in ER and consequent UPR activation, attributed to both
55 intrinsic and extrinsic factors, were documented in many human cancer types [10].

56 Irrespective of the mechanism of ER stress induction, UPR represents the main response of the cells
57 to ER stress as well as cytoprotective mechanism to cope with stress inducing conditions and to
58 restore ER homeostasis and functions [11]. UPR includes the repression of protein synthesis, the
59 degradation of the unfolded proteins by ER-associated degradation (ERAD) and the promotion of
60 appropriate protein folding mediated by ER chaperones. The expression of ER chaperones depends
61 on the activation of all three arms of UPR signaling that includes activation of the activating
62 transcription factor 6 (ATF6), protein kinase RNA-like ER kinase (PERK), and inositol-requiring
63 enzyme-1α (IRE1α) [11]. ER stress-induced cleavage of ATF6 into an active cytosolic ATF6
64 fragment p50 and its consequent translocation to the nucleus activates expression of ER chaperones
65 [12]. Despite significant reduction of overall frequency of mRNA translation initiation resulting
66 from phosphorylation of eIF2α via PERK, ATF4 mRNA is preferentially translated to active ATF4
67 that also drives the expression of ER chaperones [13]. Finally, the X-box binding protein 1 (XBP1)
68 mRNA cleavage and splicing depends on autophosphorylation of IRE1α that activates IRE1α
69 endoribonuclease. The spliced form of the transcription factor XBP1s induces expression of
70 proteins involved in ERAD [14, 15], ER chaperones and proteins facilitating protein folding [16].
71 ERAD includes retro-translocation of aberrant proteins from ER to the cytosol through the
72 membrane spanning retro-translocon [17, 18]. Aberrant proteins are further polyubiquitinated by
73 means of E3 ubiquitin ligases HRD1 and finally degraded by the 26S proteasome [18-20].
74 Activation of IRE1α can also result in cleavage of ER-localized mRNAs in a process known as
75 regulated IRE1α -dependent decay, which further decreases ER translational load and helps to
76 restore cellular homeostasis [21].

77 Despite induction of cytoprotective UPR, chronic or intensive ER stress can culminate in different
78 forms of cell death [11]. The best described ER stress-induced apoptosis depends on ATF4-
79 mediated expression of CHOP that further initiates expression of pro-apoptotic proteins PUMA and
80 Noxa [11]. Tumor cells, however, exhibit resistance to the different forms of cell death [22].
81 Previous studies have implicated UPR activation in different aspects of carcinogenesis in a variety
82 of cancer types [7, 8]. A number of small molecules were recently identified to interfere with

various arms of the UPR and ERAD, however, potential translation of this knowledge to cancer therapy has been limited to date [23, 24]. The impact of ERAD inhibitor eeyarestatin on either tumor cell survival [25] or chemotherapy sensitivity [26] was examined while the impact of LS-102, an inhibitor of enzymatic activity of HRD1 that represents the central and essential protein of ERAD [19, 20], on cancer cells survival and response was not investigated.

On the basis of previous studies, we assume that the increased rate of protein synthesis in tumor cells leads to an overload of protein quality control mechanisms including ERAD. Since ER stress and consequent UPR signaling in tumor cells could also be increased because of changes in tumor micro environment [7, 9] we hypothesize that tumor cells will be more sensitive to ERAD inhibition than normal cells. Thus, in the present study, we have examined impact of LS-102 on survival of the cells of human cell lines derived from GBM and neuroblastoma. We have used two different glioblastoma cells with opposite characteristics that are important with respect to GBM. T98G cells contain mutant-type *TP53* with positive O^6-methylguanine-DNA methyltransferase (MGMT) that is responsible for the resistance of GBM cells to temozolomide, while U87 cells contain wild-type *TP53* with negative MGMT [27]. In addition, we have investigated impact of LS-102 on neuroblastoma SH-SY5Y cells and normal human astrocytes represented by NHA and K1884 cells. We have examined molecular responses of the cells to HRD1 inhibition with a focus on expression of proteins playing an essential role in UPR and ERAD as well as on XBP1 splicing. Finally, we have also examined impact of LS-102 on p53 expression in GBM cells.

Materials and methods

Materials. The following materials were obtained commercially: sodium dodecylsulphate (SDS), bovine serum albumin (BSA), (3-(4,5-dimethylthiazol-2-yl)-2,5-diphenyltetrazolium bromide (MTT), trypsin (EC 3.4.21.4), 3-[(3-cholamidopropyl)dimethylammonio]-1-propanesulfonate hydrate (CHAPS) (AppliChem); tunicamycin (Calbiochem); LS-102 (Merck); HALT^{TM} protease inhibitor cocktail (Thermo Fisher Scientific); prestained protein standards (BioRad, #1610373); mouse monoclonal antibodies against HSP60 (#SC-271215, Santa Cruz Biotechnology), p53 (#SC-55476, Santa Cruz Biotechnology) and β-actin (#3700, Cell Signaling); rabbit polyclonal antibody against HRD1 (#13473-1-AP, Proteintech); GRP78 (#ab227865, Abcam); SEL1L (#PA5-88333, Invitrogen); LONP1 (#PA5-51692, Invitrogen); goat anti-rabbit (#A0545, Sigma-Aldrich) and goat anti-mouse (#A0168, Sigma-Aldrich) secondary antibodies conjugated with horse radish peroxidase.

Cell culture and treatment. Glioblastoma U87 cells (ATCC) and were maintained in DMEM medium (Thermo Fisher Scientific) supplemented with 10% fetal bovine serum and 1% penicillin-streptomycin (all PAA) at 37 °C and 5% CO_2 humidified atmosphere.

Glioblastoma T98G cells (ATCC) were maintained in DMEM medium (Thermo Fisher Scientific) supplemented with 10% fetal bovine serum and 1% penicillin-streptomycin (all PAA) at 37 °C and 5% CO_2 humidified atmosphere.

Primary human astrocytes K1884 (Gibco) were maintained in a specific medium for astrocyte growth (DMEM 1×, GlutaMAX, N-2 Supplement, One Shot FBS) (Thermo Fisher Scientific) at 37 °C and 5% CO_2 humidified atmosphere.

Primary human astrocytes NHA (ATCC) were maintained in MEM medium (Thermo Fisher Scientific) medium supplemented with 10% fetal bovine serum and 1% penicillin-streptomycin (all PAA) at 37 °C and 5% CO_2 humidified atmosphere.

Neuroblastoma SH-SY5Y cells (ATCC) were maintained in DMEM:F12 (1:1) medium supplemented with 10% fetal bovine serum and 1% penicillin-streptomycin (all PAA) at 37 °C and under a 5% CO_2 humidified atmosphere.

The media were changed every 3 days.

The cells were treated with the indicated concentrations of either LS-102 for 24 h at 37 °C and under a 5% CO_2 humidified atmosphere. At the end of the treatment, the cells were washed 3 times with ice-cold phosphate-buffered saline (PBS) and then re-suspended in a lysis buffer (30 mmol/l Tris-HCl, 150 mmol/l NaCl, 1% CHAPS, 1× protease inhibitor cocktail, pH=7.6) for total protein extraction. Protein concentrations were determined by a protein DC assay kit (Bio-Rad) with BSA as a standard.

Cell viability. The cells were seeded in 96-well plates at optimal concentrations. Control cells and the cells treated with LS-102 were incubated for indicated time intervals at 37 °C under a 5% CO_2 humidified atmosphere. At the end of incubation, a 0.01 ml MTT solution (5 mg/ml) was added to each well, and the cells were further incubated for 4 hours at 37 °C and under a 5% CO_2 humidified atmosphere. The insoluble formazan, which resulted from the oxidation of added MTT by vital cells, was dissolved by the addition of 0.1 ml of SDS solution (0.1 g/ml) and overnight incubation at 37 °C under a 5% CO_2 humidified atmosphere. The absorbance of formazan was determined spectrophotometrically by using a Synergy H4 microplate reader (Agilent). The relative viability of the cells was determined as the ratio of the optical density of formazan produced by treated cells to the optical density of the formazan produced by untreated control cells and was expressed as a per cent of the control. For each treatment time, the optical density value of untreated control cells was considered as 100% of viable cells.

Western blotting. Isolated proteins (30 μg proteins loaded/lane) were separated on 10% SDS-polyacrylamide gel electrophoresis (PAGE) under reducing conditions. Separated proteins were transferred to nitrocellulose membranes by using semi-dry transfer, and membranes were probed with antibodies specific to GRP78 (1:1,000), HRD1 (1:1,000), HSP60 (1:1,000), LONP1(1:1,000), SEL1L (1:1,000), p53 (1:1,000) and β-actin (1:2,000). Further incubation of the membranes with particular secondary antibodies (1:10,000 mouse, 1:20,000 rabbit) was followed by the visualization of immunopositive bands by using the chemiluminescent substrate SuperSignal West Pico (Thermo Fisher Scientific) and the Chemidoc XRS system (Bio-Rad). Intensities of specific bands were quantified by Quantity One software (Bio-Rad). The intensities of bands of interest were normalized to corresponding intensities of bands of β-actin and were expressed as the intensity of the band of the particular protein in treated cells relative to the intensity of the band in control untreated cells.

Isolation of total RNA and cDNA synthesis. Total RNA was isolated from harvested cells treated with the indicated concentrations of either LS-102 or tunicamycin at a concentration 2 μmol/l for 6 h at 37 °C using Tri reagent (MRC) following the manufacturer's protocol. Total RNA (1 μg) was reversely transcribed to cDNA by using a mRNA-MAXIMA First Strand cDNA synthesis kit (Thermo Fisher Scientific) according to the protocol supplied by the manufacturer.

Reverse-transcription polymerase chain reaction (RT-PCR). Aliquots of the resulting cDNA corresponding to 5 ng total RNA were used for PCR. Sequences of primers used for amplification of XBP1 mRNA (Table 1) were designed and verified by using the nucleotide database of the National Center for Biotechnology Information. Amplification of the cDNAs was initiated by denaturation at 95 °C for 3 min, followed by 35 PCR cycles (initial denaturation at 95 °C for 3 min followed by cycles of denaturation at 95 °C for 30 s, annealing at 58 °C for 30 s, and extension at 72 °C for 30 s) and final extension at 72 °C for 7 min in a DNA thermal cycler (Biometra). The PCR products were separated by electrophoresis in 3% agarose gel and then visualized by ethidium bromide staining.

Statistical analysis. One-way ANOVA (GraphPad InStat V2.04a, GraphPad Software) was first carried out to test for differences among all experimental groups. Additionally, Tukey's test was used to determine the differences between individual groups. A $p < 0.05$ was considered as being significant.

Results

Impact of LS-102 on relative cell viability of the cells. The testing of the relative cell viability with the MTT assay at 24, 48 and 72 h after the treatment of the cells with different concentrations

183   of LS-102 revealed a concentration-dependent reduction of the relative viability of the cells of
184   investigated cell lines (Figure 1). The IC50 values (concentrations causing decrease of the relative
185   cell viability to 50 % of control untreated cells) for used cell lines are summarized in Table 2. As
186   indicated, the cells of astrocyte cell line K1884 exhibit the highest sensitivity while the cells of
187   glioblastoma cell line T98G are the most resistant (Table 2). The kinetics of the cell death seems to
188   be fast. Although there is a trend towards decreased IC50 values with an increased time of
189   treatment, the time-dependent changes of IC50 values are not statistically significant.

190   **Impact of LS-102 on expression of proteins involved in UPR and ERAD.** In order to test the
191   impact of LS-102 on expression of proteins involved in UPR and ERAD we have performed
192   Western blot analysis of the protein extracts prepared from control untreated cells and the cells
193   treated with indicated concentrations of LS-102 for 24h. We have focused our interest on GRP78
194   that is the master protein involved in activation of UPR [11] and HRD1 that is E3 ligase involved in
195   ERAD [18]. Interaction of HRD1 with SEL1L is a prerequisite for the formation of a functional
196   HRD1-ERAD complex [28], therefore we have also analyzed impact of LS-102 on expression of
197   SEL1L. Since HRD1 is also involved in regulation of mitochondrial biogenesis [29] and dynamics
198   [30], we have also examined the impact of LS-102 on the levels of HSP60 and LONP1 that are
199   important molecular components of mitochondrial UPR [31].

200   Treatment of the T98G cells for 24 h with LS-102 at a concentration 10 μmol/l (Figure 2) was
201   associated with significant increase of expression of HRD1 (202.3% of control, $p < 0.01$), GRP78
202   (226.1% of control, $p < 0.01$) and SEL1L (187.4% of control, $p < 0.01$). After the treatment of the
203   T98G cells for 24 h with LS-102 at a concentration 5 μmol/l, the levels of HRD1, GRP78 and
204   SEL1L were elevated but the changes were not statistically significant (Figure 2). The levels of
205   HSP60 and LONP1 were not significantly changed at both investigated concentrations (Figure 2).

206   The similar results were observed after the treatment of U87 cells with LS-102 (Figure 3). We have
207   observed significantly increased levels of HRD1 (194.3% of control, $p < 0.01$), GRP78 (228.3% of
208   control, $p < 0.01$) and SEL1L (216.9% of control, $p < 0.01$) after the treatment of the U87 cells for
209   24 h with LS-102 at a concentration 5 μmol/l while the levels of HRD1, GRP78 and SEL1L were
210   not significantly increased after the treatment of the U87 cells for 24 h with LS-102 at a
211   concentration 2.5 μmol/l (Figure 3). The levels of HSP60 and LONP1 were not significantly
212   changed at both investigated concentrations (Figure 3).

213   The levels of all investigated proteins were not significantly changed after the treatment of both SH-
214   SY5Y (Figure 4) and K1884 (Figure 4) cells for 24 h with indicated concentrations of LS-102.

215   **Impact of LS-102 on splicing of XBP1 mRNA.** In order to test the impact of LS-102 on activation
216   of IRE1α-XBP1 axis of UPR, we have treated the cells with different concentrations of LS-102

217 followed with RT-PCR analysis of RNA isolated from control untreated cells and cells treated with
218 LS-102 for 6 h. The time interval was selected on the basis of our previous publications [15, 32]. In
219 addition, RNA isolated from the cells treated with tunicamycin at a concentration of 2 μmol/l for 6
220 h has also been analyzed serving as a positive control. In agreement with our previous studies [15,
221 32], treatment of all cells with tunicamycin was associated with splicing of XBP1 mRNA (Figure
222 5). Treatment of the cells with LS-102 induced splicing of XBP1 mRNA in T98G and K1884 cells
223 while the splicing of XBP1 mRNA was not observed after the treatment of SH-SY5Y and U87 cells
224 with indicated concentrations of LS-102 (Figure 5).

225 **Impact of LS-102 on p53 expression in glioblastoma cells.** In order to explain differential
226 sensitivity of GBM cells to LS-102 we have performed WB analysis of p53 expression in U87 and
227 T98G cells since it was documented earlier that HRD1 targets p53 for ubiquitination and further
228 destruction [33]. In accordance with a generally accepted view that mutant p53 is stable, we have
229 documented significantly stronger signal of p53 in T98G cells as compared to the signal of p53 in
230 U87 cells (Figure 6). Treatment of U87 cell with LS-102 was not associated with elevated
231 expression of p53 (Figure 6). In addition, treatment of U87 cell with LS-102 was not associated
232 with activation of caspase 3 (Supplementary Figure S1).

233

234 **Discussion**
235 In this study, we have documented the sensitivity of different cell types derived from GBM,
236 neuroblastoma and normal astrocytes to the inhibitor of HRD1 enzymatic activity LS-102. With
237 respect to GBM cells, U87 cells are very sensitive to LS-102 while T98G cells are less sensitive to
238 the inhibition of HRD1 function. Cells of cell lines derived from normal astrocytes exhibit also
239 differential sensitivity to LS-102. K1884 cells exhibit the highest sensitivity to LS-102 among all
240 cell types used in the study while NHA cells are the most resistant. Sensitivity of neuroblastoma
241 SH-SY5Y cells to LS-102 is comparable to the sensitivity of U87 cells. In addition, we have shown
242 that inhibition of HRD1 has differential impact on induction of expression of HRD1, SEL1L and
243 GRP78 as well as on XBP1 mRNA splicing.

244 HRD1 is ER resident E3 ligase playing an essential role in the process of ERAD [17, 18] that is
245 important mechanism of the quality control of secretory pathway proteins. Inhibitors of HRD1 were
246 designed as novel candidates for the treatment of rheumatoid arthritis [34] but their effectivity to
247 kill malignant cells is less described [23]. In our previous study, we have shown that expression of
248 HRD1 depends on ribonuclease activity of IRE1α that results in splicing of XBP1 mRNA [15]. In
249 glioblastoma cells T98G and U87, the inhibition of HRD1 activity was associated with increased
250 expression of HRD1, SEL1L and GRP78. While in T98G cells increased expression of HRD1 after

251 the treatment of the cells with LS-102 correlates well with the activation of IRE1α documented by

252 XBP1 splicing, the expression of HRD1 after treatment of both U87 and K1884 cells with LS-102

253 does not correlate with activation of IRE1α. In U87 cells, inhibition of HRD1 resulted in increased

254 expression of HRD1 but was not associated with splicing of XBP1. On contrary, inhibition of

255 HRD1 does not result in increased expression of HRD1 in K1884 cells despite documented splicing

256 of XBP1. Thus, the results presented in this study do not indicate the sole relationship between

257 IRE1α activity and expression of HRD1. It seems that relationship between HRD1 activity and

258 expression of either GRP78 or SEL1L is even more complex. In response to ER stress, upregulation

259 of SEL1L involves activation ATF6 branch of UPR while expression of HRD1 depends on

260 activation of IRE1-dependent splicing of XBP1 [15]. With respect to ERAD, the recent study

261 documented that downregulation of HRD1 was associated with increased expression of SEL1L in

262 the cells of macrophage cell line RAW 264.7 [35]. These results and results presented in our study

263 indicate possible association between HRD1 activity/level and expression of SEL1L. On contrary,

264 downregulation of SEL1L resulted in decreased expression of HRD1 in both HEK239T cells [28]

265 and bone marrow-derived macrophages of myeloid cell-specific *Sel1L*-deficient mice [35].

266 Interestingly, expression of GRP78 in bone marrow-derived macrophages of myeloid cell-specific

267 *Sel1L*-deficient mice was increased [35]. In response to ER stress, expression of GRP78 is regulated

268 by PERK-ATF4 branch of UPR [36]. The previously published results together with results of our

269 study indicate that the regulation of expression of critical molecular components of both UPR and

270 ERAD is more complex and cell specific but the mechanism of increased expression of HRD1,

271 GRP78 and SEL1L after inhibition of HRD1 is unclear. Increased expression of GRP78 correlates

272 well with tumor characteristics and was documented in GBM upon recurrence [37]. Over-

273 expression of both HRD1 and GRP78 is considered to be cytoprotective [38] or associated with

274 aggressive growth and invasive properties of cancer cells [39]. In GBM cells, it might represent

275 compensatory intracellular mechanism to cope with HRD1 inhibition and should confer some

276 resistance to cell death. Despite similar molecular responses of both T98G and U87 cells to the

277 inhibition of HRD1, the sensitivity of the GBM cells to LS-102 was significantly different.

278 Differential sensitivity of GBM cells to LS-102 might be also attributed to the fact that resistant

279 T98G cells are expressing mutant form of p53 while sensitive U87 cells are expressing wild type of

280 p53 [27]. It was documented earlier that HRD1 targets p53 for ubiquitination and further

281 destruction [33]. Since we did not observe induction of p53 in U87 cells treated with LS-102 we

282 presume that p53-dependent apoptosis is not a mechanism of death of GBM cells induced by LS-

283 102. Thus, the mechanism of differential sensitivity of GBM cells to LS-102 is not clear but it is not

284 dependent on cellular status of *TP53* gene and p53-induced apoptosis.

In conclusion, we have shown that inhibition of HRD1 enzymatic activity by micromolar concentrations of LS-102 is associated with a fast death of the cells of all cell lines used in the study. The impact of LS-102 on XBP1 splicing and expression of HRD1, SEL1L and GRP78 was specific to GBM cells but does not correlate with sensitivity of the cells to LS-102. Since LS-102 induces also death of normal astrocytes it is not a candidate for the testing of its potential use as a treatment of GBM.

Supplementary data are available in the online version of the paper.

References

[1] DAVIS ME. Epidemiology and Overview of Gliomas. Semin Oncol Nurs 2018; 34: 420-429. https://doi.org/10.1016/j.soncn.2018.10.001

[2] WEATHERS SP, GILBERT MR. Advances in treating glioblastoma. F1000Prime Rep 2014; 6: 46. https://doi.org/10.12703/P6-46

[3] LAH TT, NOVAK M, BREZNIK B. Brain malignancies: Glioblastoma and brain metastases. Semin Cancer Biol 2020; 60: 262-273. https://doi.org/10.1016/j.semcancer.2019.10.010

[4] BROOKS LJ, CLEMENTS MP, BURDEN JJ, KOCHER D, RICHARDS L et al. The white matter is a pro-differentiative niche for glioblastoma. Nat Commun 2021; 12: 2184. https://doi.org/10.1038/s41467-021-22225-w

[5] VEHLOW A, CORDES N. Invasion as target for therapy of glioblastoma multiforme. Biochim Biophys Acta 2013; 1836: 236-244. https://doi.org/10.1016/j.bbcan.2013.07.001

[6] CUDDAPAH VA, ROBEL S, WATKINS S, SONTHEIMER H. A neurocentric perspective on glioma invasion. Nat Rev Neurosci 2014; 15: 455-465. https://doi.org/10.1038/nrn3765

[7] CHEN X, CUBILLOS-RUIZ JR. Endoplasmic reticulum stress signals in the tumour and its microenvironment. Nat Rev Cancer 2021; 21: 71-88. https://doi.org/10.1038/s41568-020-00312-2

[8] OAKES SA. Endoplasmic Reticulum Stress Signaling in Cancer Cells. Am J Pathol 2020; 190: 934-946. https://doi.org/10.1016/j.ajpath.2020.01.010

[9] BARTOSZEWSKA S, COLLAWN JF, BARTOSZEWSKI R. The Role of the Hypoxia-Related Unfolded Protein Response (UPR) in the Tumor Microenvironment. Cancers (Basel) 2022; 14: 4870. https://doi.org/10.3390/cancers14194870

[10] MADDEN E, LOGUE SE, HEALY SJ, MANIE S, SAMALI A. The role of the unfolded protein response in cancer progression: From oncogenesis to chemoresistance. Biol Cell 2019; 111: 1-17. https://doi.org/10.1111/boc.201800050

[11] ALMANZA A, CARLESSO A, CHINTHA C, CREEDICAN S, DOULTSINOS D et al. Endoplasmic reticulum stress signalling - from basic mechanisms to clinical applications. FEBS J 2019; 286: 241-278. https://doi.org/10.1111/febs.14608

[12] YOSHIDA H, OKADA T, HAZE K. ATF6 activated by proteolysis binds in the presence of NF-Y (CBF) directly to the cis-acting element responsible for the mammalian unfolded

330   protein response. Mol Cell Biol 2000; 20: 6755-6767.
331   https://doi.org/10.1128/MCB.20.18.6755-6767.2000

332 [13] HARDING HP, ZHANG Y, BERTOLOTTI A, ZENG H, RON D. Perk is essential for
333   translational regulation and cell survival during the unfolded protein response. Mol Cell
334   2000; 5: 897-904. https://doi.org/10.1016/s1097-2765(00)80330-5

335 [14] KANEKO M, YASUI S, NIINUMA Y, OMURA T, OKUMA Y et al. A different pathway
336   in the endoplasmic reticulum stress-induced expression of human HRD1 and SEL1 genes.
337   FEBS Lett 2007; 581: 5355-5360. https://doi.org/10.1016/j.febslet.2007.10.033

338 [15] DIBDIAKOVA K, SAKSONOVA S, PILCHOVA I, KLACANOVA K, TATARKOVA Z
339   et al. Both thapsigargin- and tunicamycin-induced endoplasmic reticulum stress increases
340   expression of Hrd1 in IRE1-dependent fashion. Neurol Res 2019; 41: 177-188.
341   https://doi.org/10.1080/01616412.2018.1547856

342 [16] LEE AH, IWAKOSHI NN, GLIMCHER LH. XBP-1 regulates a subset of endoplasmic
343   reticulum resident chaperone genes in the unfolded protein response. Mol Cell Biol 2003;
344   23: 7448-7459. https://doi.org/10.1128/MCB.23.21.7448-7459.2003

345 [17] HAMPTON RY, SOMMER T. Finding the will and the way of ERAD substrate
346   retrotranslocation. Curr Opin Cell Biol 2012; 24: 460-466.
347   https://doi.org/10.1016/j.ceb.2012.05.010

348 [18] CHRISTIANSON JC, JAROSCH E, SOMMER T. Mechanisms of substrate processing
349   during ER-associated protein degradation. Nat Rev Mol Cell Biol 2023; 24: 777-796.
350   https://doi.org/10.1038/s41580-023-00633-8

351 [19] KIKKERT M, DOOLMAN R, DAI M, AVNER R, HASSINK G et al. Human HRD1 is an
352   E3 ubiquitin ligase involved in degradation of proteins from the endoplasmic reticulum. J
353   Biol Chem 2004; 279: 3525-3534. https://doi.org/10.1074/jbc.M307453200

354 [20] PRESTON GM, BRODSKY JL. The evolving role of ubiquitin modification in endoplasmic
355   reticulum-associated degradation. Biochem J 2017; 474: 445-469.
356   https://doi.org/10.1042/BCJ20160582

357 [21] HOLLIEN J, LIN JH, LI H, STEVENS N, WALTER P et al. Regulated Ire1-dependent
358   decay of messenger RNAs in mammalian cells. J Cell Biol 2009; 186: 323-331.
359   https://doi.org/10.1083/jcb.200903014

360 [22] HANAHAN D, WEINBERG RA. Hallmarks of cancer: the next generation. Cell 2011; 144:
361   646-674. https://doi.org/10.1016/j.cell.2011.02.013

362 [23] MARCINIAK SJ, CHAMBERS JE, RON D. Pharmacological targeting of endoplasmic
363   reticulum stress in disease. Nat Rev Drug Discov 2022; 212: 115-140.
364   https://doi.org/10.1038/s41573-021-00320-3

365 [24] KARAMALI N, EBRAHIMNEZHAD S, KHALEGHI MOGHADAM R, DANESHFAR N,
366   REZAIEMANESH A. HRD1 in human malignant neoplasms: Molecular mechanisms and
367   novel therapeutic strategy for cancer. Life Sci 2022; 301: 120620.
368   https://doi.org/10.1016/j.lfs.2022.120620

369 [25] WANG Q, MORA-JENSEN H, WENIGER MA, PEREZ-GALAN P, WOLFORD C et al.
370   ERAD inhibitors integrate ER stress with an epigenetic mechanism to activate BH3-only
371   protein NOXA in cancer cells. Proc Natl Acad Sci U S A 2009; 106: 2200-2205.
372   https://doi.org/10.1073/pnas.0807611106

373 [26] BREM GJ, MYLONAS I, BRÜNING A. Eeyarestatin causes cervical cancer cell
374   sensitization to bortezomib treatment by augmenting ER stress and CHOP expression.
375   Gynecol Oncol 2013; 128: 383-390. https://doi.org/10.1016/j.ygyno.2012.10.021

376 [27] WANG X, CHEN JX, LIU YH, YOU C, MAO Q. Mutant TP53 enhances the resistance of
377   glioblastoma cells to temozolomide by up-regulating O(6)-methylguanine DNA-
378   methyltransferase. Neurol Sci 2013; 34: 1421-1428. https://doi.org/10.1007/s10072-012-
379   1257-9

380 [28] LIN LL, WANG HH, PEDERSON B, WEI X, TORRES M et al. SEL1L-HRD1 interaction
381   is required to form a functional HRD1 ERAD complex. Nat Commun 2024; 17: 1440.
382   https://doi.org/10.1038/s41467-024-45633-0
383 [29] FUJITA H, YAGISHITA N, ARATANI S, SAITO-FUJITA T, MOROTA S, et al. The E3
384   ligase synoviolin controls body weight and mitochondrial biogenesis through negative
385   regulation   of   PGC-1β.   EMBO   J   2015;   34:   1042-1055.
386   https://doi.org/10.15252/embj.201489897.
387 [30] ZHOU Z, TORRES M, SHA H, HALBROOK CJ, VAN DEN BERGH F et al. Endoplasmic
388   reticulum-associated degradation regulates mitochondrial dynamics in brown adipocytes.
389   Science 2020; 368: 54-60. https://doi.org/10.1126/science.aay2494
390 [31] FIORESE CJ, SCHULZ AM, LIN YF, ROSIN N, PELLEGRINO MW et al. 2016 The
391   Transcription Factor ATF5 Mediates a Mammalian Mitochondrial UPR. Curr Biol 2016; 26:
392   2037-2043. https://doi.org/10.1016/j.cub.2016.06.002
393 [32] BRODNANOVA M, HATOKOVA Z, EVINOVA A, CIBULKA M, RACAY P.
394   Differential impact of imipramine on thapsigargin- and tunicamycin-induced endoplasmic
395   reticulum stress and mitochondrial dysfunction in neuroblastoma SH-SY5Y cells. Eur J
396   Pharmacol 2021; 902: 174073. https://doi.org/10.1016/j.ejphar.2021.174073
397 [33] YAMASAKI S, YAGISHITA N, SASAKI T, NAKAZAWA M, KATO Y et al.
398   Cytoplasmic destruction of p53 by the endoplasmic reticulum-resident ubiquitin ligase
399   'Synoviolin'. EMBO J 2007; 26: 113-122. https://doi.org/10.1038/sj.emboj.7601490
400 [34] YAGISHITA N, ARATANI S, LEACH C, AMANO T, YAMANO Y et al. RING-finger
401   type E3 ubiquitin ligase inhibitors as novel candidates for the treatment of rheumatoid
402   arthritis. Int J Mol Med 2012; 30: 1281-1286. https://doi.org/10.3892/ijmm.2012.1129
403 [35] JI Y, LUO Y, WU Y, ZHAO L, XUE Z et al. SEL1L-HRD1 endoplasmic reticulum-
404   associated degradation controls STING-mediated innate immunity by limiting the size of the
405   activable STING pool. Nat Cell Biol 2023; 25: 726-739. https://doi.org/10.1038/s41556-
406   023-01138-4
407 [36] LUO S, BAUMEISTER P, YANG S. ABCOUWER SF, LEE AS. Induction of Grp78/BiP
408   by translational block: activation of the Grp78 promoter by ATF4 through and upstream
409   ATF/CRE site independent of the endoplasmic reticulum stress elements. J Biol Chem 2003;
410   278: 37375-37385. https://doi.org/10.1074/jbc.M303619200
411 [37] LIU K, TSUNG K, ATTENELLO FJ. Characterizing Cell Stress and GRP78 in Glioma to
412   Enhance   Tumor   Treatment.   Front   Oncol   2020;   10:   608911.
413   https://doi.org/10.3389/fonc.2020.608911
414 [38] OMURA T, MATSUDA H, NOMURA L, IMAI S, DENDA M et al. Ubiquitin ligase
415   HMG-CoA reductase degradation 1 (HRD1) prevents cell death in a cellular model of
416   Parkinson's   disease.   Biochem   Biophys   Res   Commun   2018;   506:   516-521.
417   https://doi.org/10.1016/j.bbrc.2018.10.094
418 [39] LEE A. Glucose-regulated proteins in cancer: molecular mechanisms and therapeutic
419   potential. Nat Rev Cancer 2014; 14: 263-276. https://doi.org/10.1038/nrc3701
420

421 **Figure Legends**

422

423 **Figure 1.** Impact of LS-102 on relative cell viability. U87, T98G, K1884, NHA and SH-SY5Y cells

424 were treated with the indicated concentrations of LS-102 for 24, 48 and 72h, and then the relative

425 viability was determined by MTT test as described in Material and methods. Data are presented as

426 means±SEM (4 independent experiments performed in triplicate per each treatment).

427

428 **Figure 2.** Impact of LS-102 on expression of HRD1, GRP78, SEL1L, HSP60 and LONP1 in T98G

429 cells. Total cell extracts were prepared from T98G cells after treatment with LS-102 at

430 concentrations 5 and 10 μM. The effect of the treatment on the levels of HRD1, GRP78, SEL1L,

431 HSP60 and LONP1 was evaluated by Western blot analysis of total cell extracts as described in

432 Materials and methods. β-actin served as the loading control. The representative blots are cropped

433 from different parts of the same blot.

434 The levels of HRD1, GRP78 and SEL1L were normalized to β-actin levels and are expressed as

435 relative to untreated controls. Data are presented as means±SD (4 independent experiments per each

436 cell line, each treatment, and each time interval). **$p < 0.01$ (one-way ANOVA, followed by

437 Tukey's test to determine differences between the protein levels in control untreated cells and

438 treated cells).

439

440 **Figure 3.** Impact of LS-102 on expression of HRD1, GRP78, SEL1L, HSP60 and LONP1 in U87

441 cells. Total cell extracts were prepared from U87 cells after treatment with LS-102 at concentration

442 2.5 and 5 μM. The effect of the treatment on the levels of HRD1, GRP78, SEL1L, HSP60 and

443 LONP1 was evaluated by Western blot analysis of total cell extracts as described in Materials and

444 Methods. β-actin served as the loading control. The representative blots are cropped from different

445 parts of same blot.

446 The levels of HRD1, GRP78 and SEL1L were normalized to β-actin levels and are expressed as

447 relative to untreated controls. Data are presented as means±SD (4 independent experiments per each

448 cell line, each treatment, and each time interval). **$p < 0.01$ (one-way ANOVA, followed by

449 Tukey's test to determine differences between the protein levels in control untreated cells and

450 treated cells).

451

452 **Figure 4.** Impact of LS-102 on expression of HRD1, GRP78, SEL1L, HSP60 and LONP1 in SH-

453 SY5Y and K1884 cells. Total cell extracts were prepared from SH-SY5Y and K1884 cells after

454 treatment with LS-102 at concentrations 2.5 and 5 μM. The effect of the treatment on the levels of

455 HRD1, GRP78, SEL1L, HSP60 and LONP1 was evaluated by Western blot analysis of total cell

456 extracts as described in Materials and methods. β-actin served as the loading control. The

457 representative blots are cropped from different parts of the same blot.

458

459 **Figure 5.** Impact of LS-102 on XBP1 splicing. Total RNA was isolated from T98G, SH-SY5Y,

460 U87 and K1884 cells treated with indicated concentrations of LS-102 or tunicamycin (TM) at a

461 concentration 2 μmol/l for 6 h. XBP1 splicing was evaluated by RT-PCR followed by agarose gel

462 electrophoresis as described in Materials and methods. L-ladder, NC-negative control, no cDNA
463 added in reaction mixture.

464

465 **Figure 6.** Impact of LS-102 on p53 expression in glioblastoma cells. Total cell extracts were
466 prepared from T98G and U87 cells after treatment with indicated concentrations of LS-102. The
467 effect of the treatment on the level of p53 was evaluated by Western blot analysis of total cell
468 extracts as described in Materials and methods. β-actin served as the loading control. The
469 representative blots are cropped from different parts of the same blot.

470

471 **Table 1.** Sequences of oligonucleotides used as primers for RT-PCR.

Gene	Forward primer	Reverse primer
XBP1	CCTGGTTGCTGAAGAGGAGG	CCATGGGGAGATGTTCTGGA

472

473   **Table 2.** IC50 values of LS-102 for different cell lines.

	IC50 (µmol/l)		
	24 h	**48 h**	**72 h**
SH-SY5Y	9.81±0.85	8.20±0.49	7.68±0.12
T98G	16.12±0.91	15.15±0.86	14.55±0.73
U87	8.51±0.81	8.05±0.34	7.55±0.71
NHA	16.59±0.62	16.45±0.35	16.08±0.43
K1884	6.61±1.32	5.18±1.61	5.14±1.72

474

Fig. 1 [Download full resolution image](#)
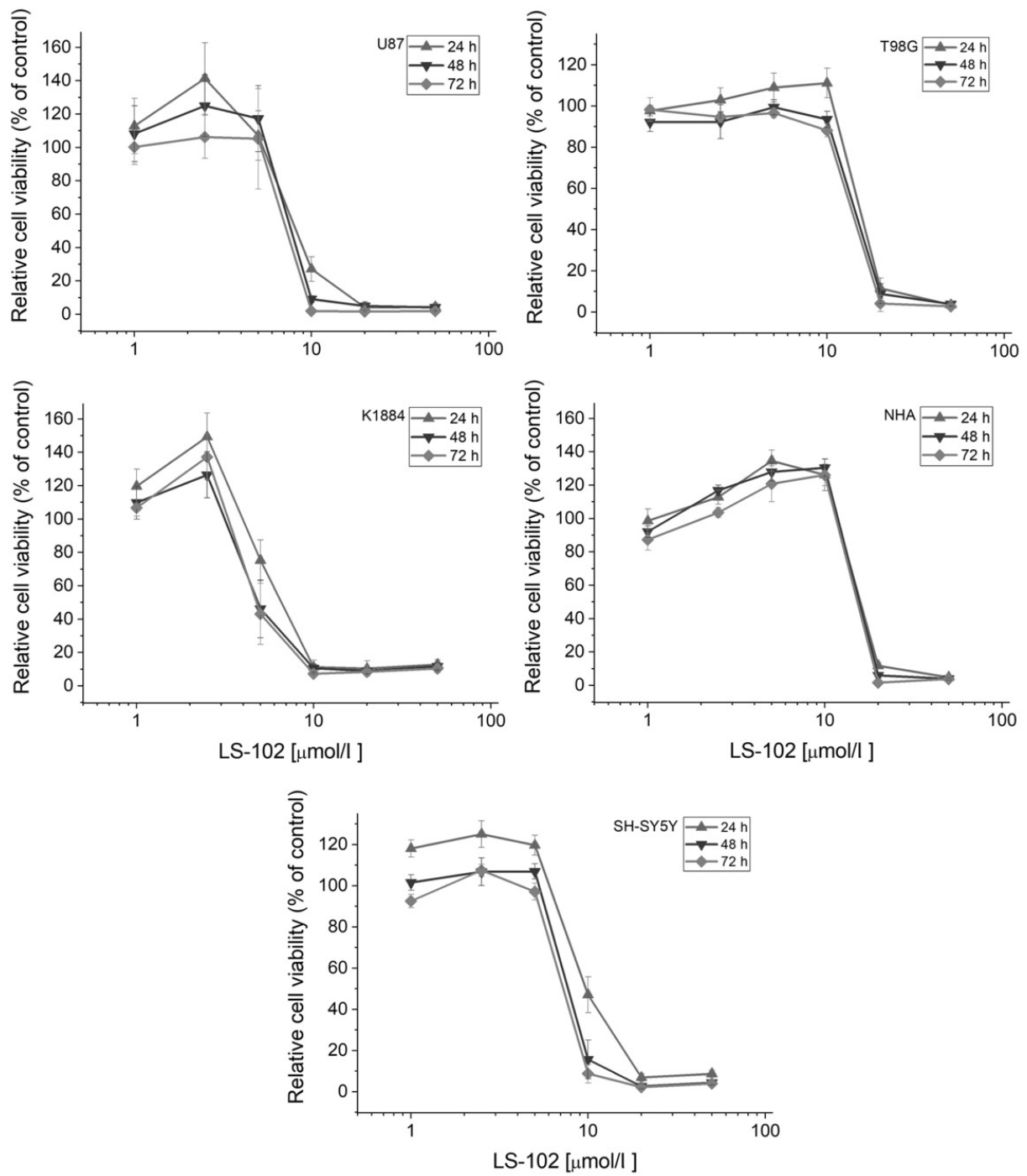
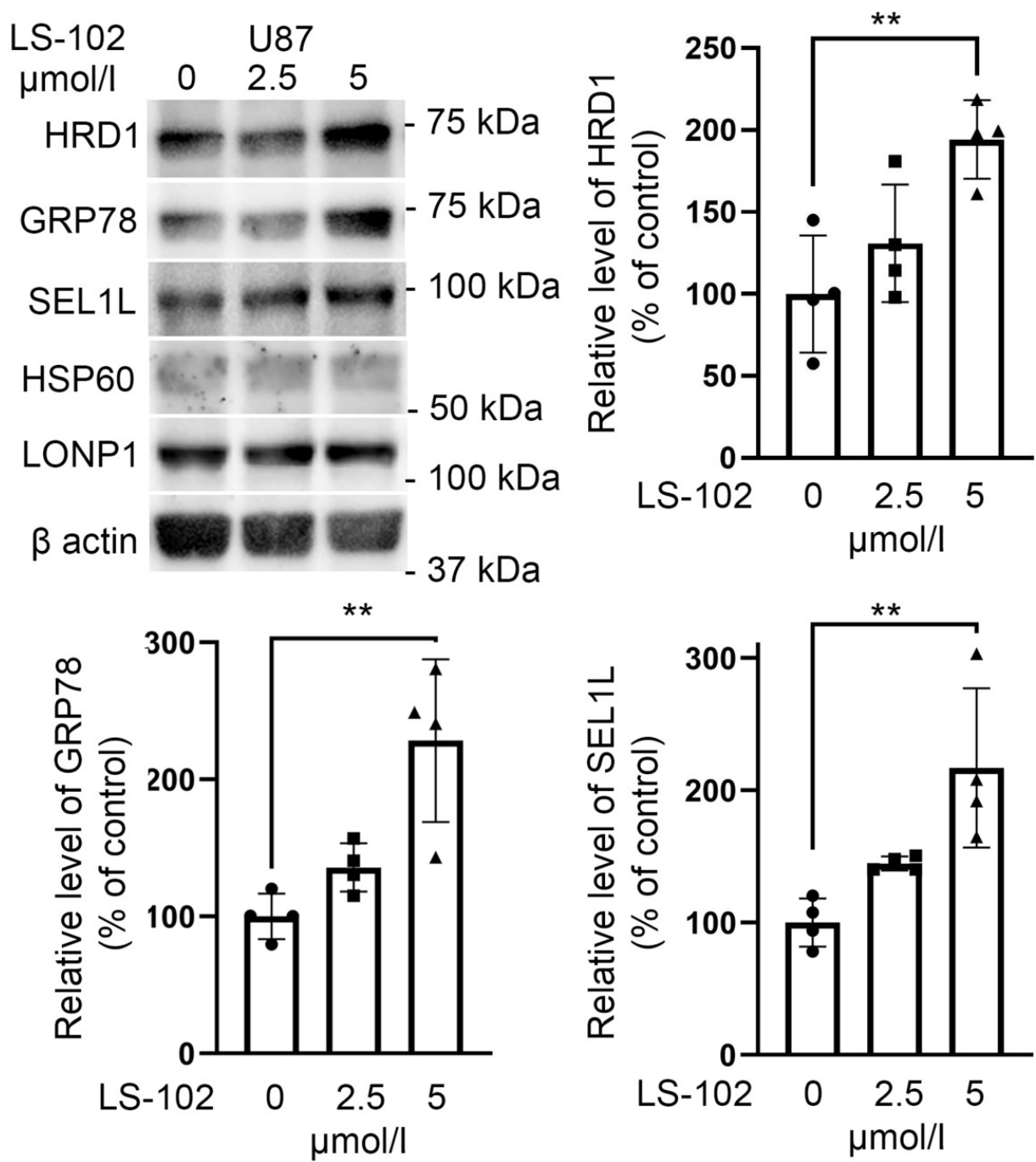Fig. 2   Download full resolution image
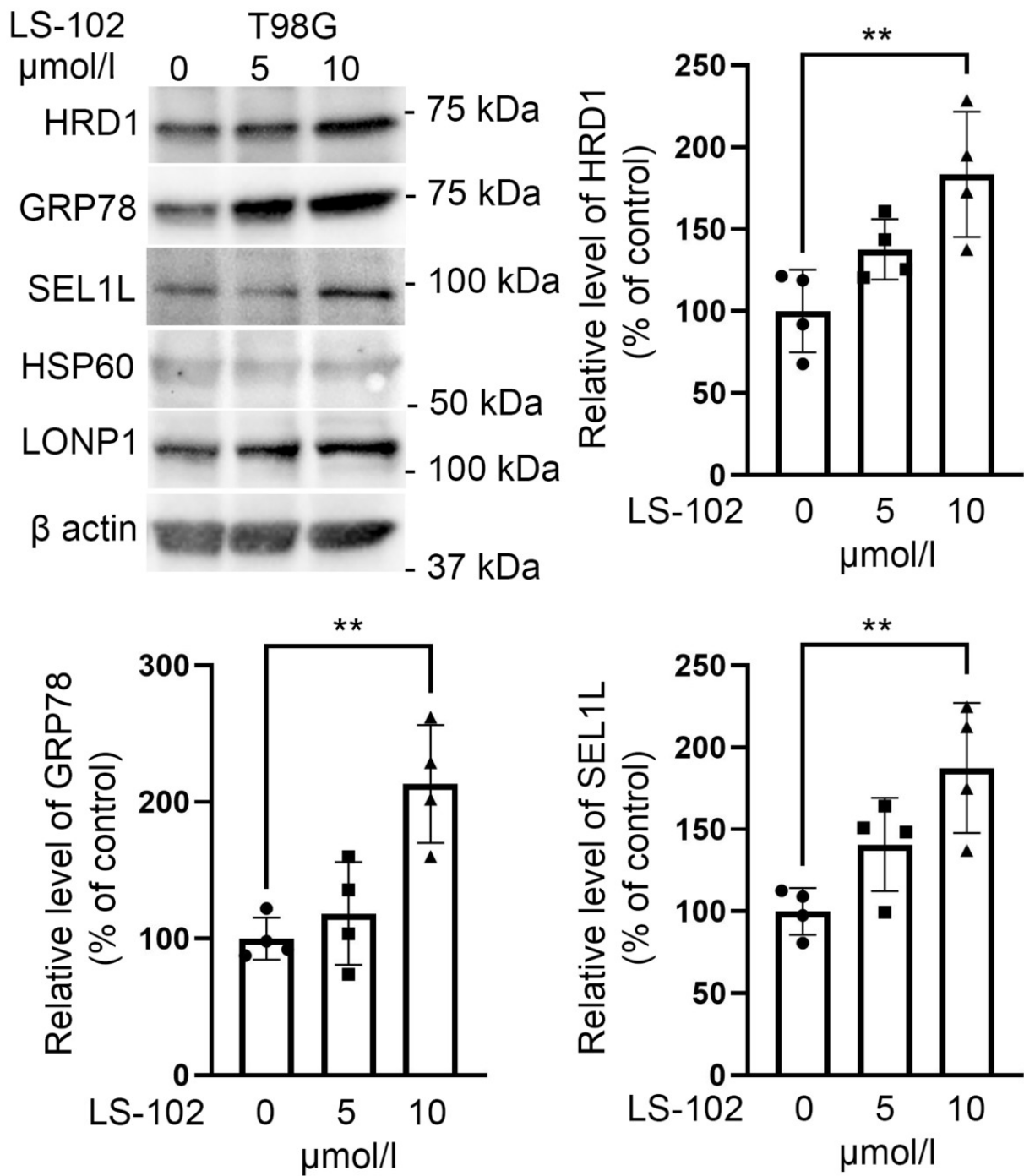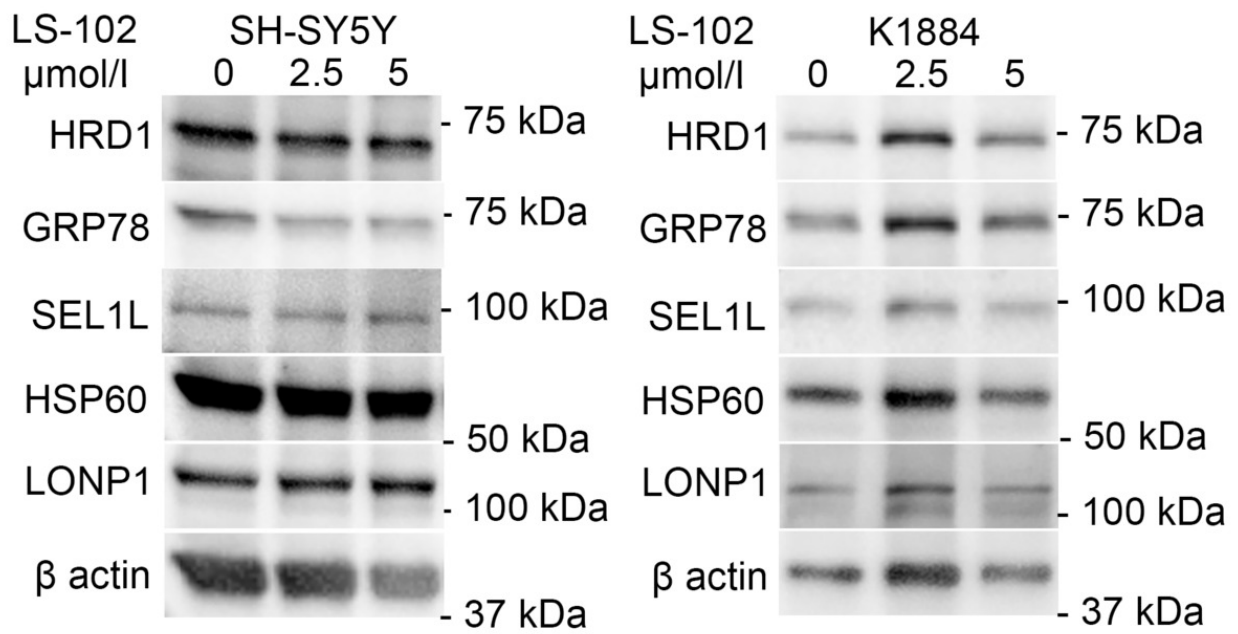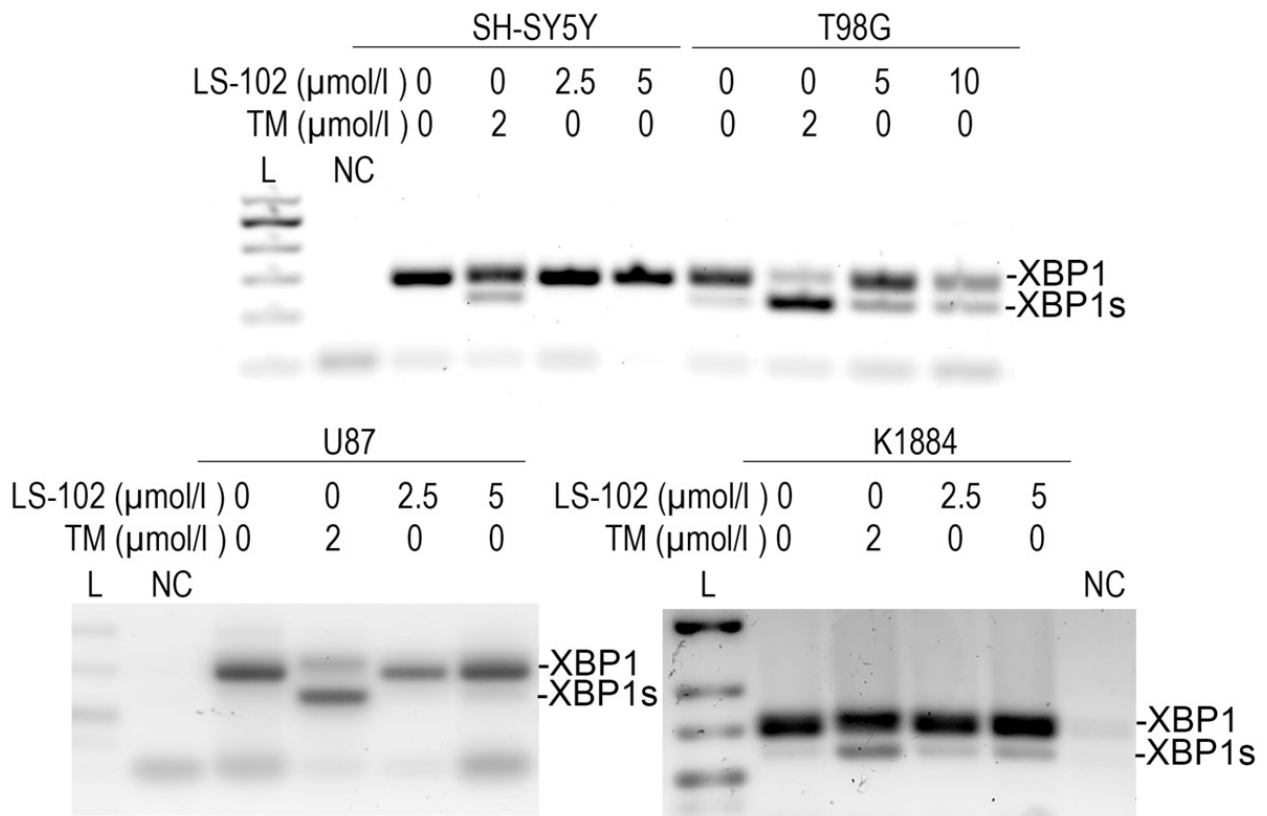
Fig. 3

Fig. 4   Download full resolution image

Fig. 5 [Download full resolution image](#)

Fig. 6   Download full resolution image